Supporting Information

D'Anjou et al. 10.1073/pnas.1212730109

SI Text

Chronology. The chronology for the composite 7,300-y record was established using five accelerator mass spectrometry (AMS) radiocarbon measurements and was further constrained by tephrochronology. Radiocarbon measurements were made on three macrofossils picked from the long sediment cores (LILA09 and LILB09) and two from the 45-cm-long surface core (LILC09) (Table S1). The sediment cores were initially placed on the same depth scale by matching up magnetic susceptibility profiles (Fig. S1). All radiocarbon ages were calibrated to calendar years using Calib, version 6.1 (1), using the IntCal09 data set (2) (Table S1).

Tephra grains isolated by acid digestion and heavy-liquid separation procedures were mounted on glass slides using EPOthin epoxy resin. Slides were scanned using a plane-polarized light microscope at a total magnification of 100–400×, allowing tephra to be differentiated from the remaining minerogenic material (3). Tephra were identified based on a grain isotropism, shape, vesicularity, and color. Seven sample were selected for geochemical analyses, where there seemed to be a clear peak in tephra concentration (0-1, 6–7, 8–9, 18–19, 23–24, 26–27, and 34–35 cm) (Fig. 2). Major element geochemistry for each horizon was determined by electron microprobe analyses using a Cameca SX50 electron microprobe, with an accelerating voltage of 15 keV, a beam current of 10 nA, and beam size of 7–10 μm. Care was taken to minimize alkali migration using shorter counting times and a defocused beam. Instrument calibration was performed using a series of silicate minerals, synthetic oxides, and glass standards. Samples yielding totals of less than 95% have been omitted (4). Geochemical results from the seven samples, where distinct peaks in shard concentrations occur, show that their compositions resemble tephra previously identified throughout the region (Table S2) as follows:

Tephra isolated from 0 to 1 cm appear to be the same as the Askja AD 1875 tephra that has been found throughout Sweden (5–7) and in a peat from Lofoten (8). These tephra can be confidently identified as the Askja AD 1875 tephra because of its distinguishing concentrations of MgO and TiO_2 (9) (Table S2).

Tephra isolated from the 6- to 7-cm depth interval contain the highest concentration of grains identified in core LILC09 (Fig. 2). Of the 37 grains analyzed from this sample, 32 tephra grains are similar to the AD 1158 eruption of Hekla (Table S2). Analytic results show little geochemical variability among grains, which are characteristic of the well-studied AD 1158 eruption (3, 9).

The 8- to 9-cm depth interval contained the second highest concentration of tephra in the core (Fig. 2). We analyzed 26 grains from this sample, and 21 grains resemble the AD 1104 eruption of Hekla, whereas the remaining 5 grains are likely from the later AD 1158 Hekla eruption (Table S2). Tephra from these eruptions are ubiquitous throughout the North Atlantic region (3, 8–13).

The 19-cm depth interval contains a mix of tephra with at least three potential sources. The geochemistry is similar to tephra identified as OWB-105 (3), BIP-24a (8), and AD 860 AD Layer B (3, 11). These eruptions are not as widespread and the mix of pollutions indicate reworking of the tephra grains prior to deposition or potentially vertical migration in the sediment sequence.

Tephra analyzed in the 27- to 28- and 35- to 36-cm samples were geochemically similar to the tephra SN-1 and QUB-565, respectively; however, they are not well documented eruptions and have large uncertainties in their age estimates so were not included in our age model (Table S2). The SN-1 tephra is dated to ∼1,775 ± 45 (14), and this age is in accordance with our age–depth model, which gives an extrapolated date of 1,766 ± 75 cal y BP. The QUB-565 date estimates are very poorly constrained but have been assigned an age of ∼2,050-2,450 calendar years before 1950 AD [calendar years before present (cal y BP)] (8). The lower end of this range (∼2,050 cal y BP) seems to be more appropriate as our age–depth model would assign a date of 2,050 ± 76 cal y BP to this depth interval. Therefore, despite large age uncertainties reported in previous studies, these ages do confirm the trends in our chronology.

An age–depth model for the composite sediment record was constructed using all of the radiocarbon dates and tephra ages from the three best established and historically dated tephra (Askja 1875, Hekla 1158, Hekla 1104). The average 2-σ uncertainty is ±63.1 y from 104 to 2,380 cal y BP and ±99.75 y from 2,380 to 7,168 cal y BP. This age–depth relationship is supported by our tentative interpretations of the other four tephra horizons identified in the upper 45 cm (Fig. 2). Radiocarbon and tephra dates are reported throughout the text as calendar years before 1950 AD (cal y BP), unless otherwise noted.

Molecular Markers and Associated Indices. Aliphatic hydrocarbons (*n*-alkanes) are widespread biomarkers in lacustrine sedimentary archives and have been intensively studied as indicators of source organisms (15–20). The principal sources of biogenic aliphatic hydrocarbons to lake sediments are algae, bacteria, and vascular plants that live within a lake, and vascular plants that live around it. Short-chained, even-numbered, C12–C22 *n*-alkanes are attributed to bacteria (18), *n*-alkanes C15–C21 (especially C17) are attributed to algae and photosynthetic bacteria (16, 20), submerged aquatic plants are the main producers of C21, C23, and C25 *n*-alkanes (19), whereas long-chained homologs (C25–C33) having an odd-over-even predominance are characteristic of higher order terrestrial plants (15) with major constituents being C27–C29 for leafy vegetation (16) and C31 for land grasses (17). Using this rationale, several studies have successfully applied ratios of these various *n*-alkane chain lengths to sedimentary records as a recorder of changes in the relative amounts of each specific source type, allowing the reconstruction of vegetation dynamics throughout the catchment. Ratios such as $[([C_{27}]+[C_{29}])/([C_{29}]+[C_{31}])]$ (21) and mean carbon number $[(MCN \text{ for C25 to C31}) = \sum([Ci]^*Ci)/\sum[Ci]]$ (22) have been shown to closely correspond with the percentage of pollen derived from grass in the sediments, revealing transitions from forested to grassland-dominated landscapes. By applying a ratio of *n*-alkanes produced mainly by tree leaf waxes to those produced by grasses $[([C_{25}] + [C_{27}] + [C_{29}])/([C_{29}] + [C_{31}])]$, we reconstruct the relative changes in composition of the terrestrial vegetation surrounding the lake, revealing transitions between a forest and a grassland-dominated system.

Pyrolytic polycyclic aromatic hydrocarbons (PAHs) are directly produced by the incomplete combustion of organic material such as terrestrial vegetation. In areas where natural forest fires are rare, these compounds can be used to explore the timing and extent of agricultural land clearance practices, or hearth development around the lake catchment. GC-MS analysis of the aromatic fractions (F2) in our sediment samples identified the PAHs; pyrene, benzo[e]pyrene, benzo[ghi]perylene, fluoranthene, and benzofluoranthene. These PAHs are known to be of pyrolytic origins and are typically associated with the combustion of terrestrial

vegetation such as trees, shrubs, grasses, and peats (23–25). Here, we report the sum of all identified pyrolytic PAHs (Total PAHs = pyrene + benzo[e]pyrene + benzo[ghi]perylene + fluoranthene + benzofluoranthenes) as a proxy for the burning of organic material originating from within the catchment area of Lilandsvatnet.

Fecal 5β-stanols and related stanol compounds (coprostanol, 5β-campestanol, 5β-stigmastanol) were chosen as biomarkers for this study due to their consistently high concentrations in the feces of humans and ruminant livestock (26, 27). Additionally, these compounds are not known to occur in any other organic materials (plant and animal) or as degradation products. Several studies have successfully applied fecal 5β-stanols and ratios of stanol compounds to mark the presence of humans or domesticated animals (cows and sheep) as well as to quantify the relative inputs from each source (26, 28, 29). Evershed and Bethell (29) proposed the use of the coprostanol:5β-stigmastanol ratio as a useful index by which human fecal deposition and that of ruminants (sheep and cows) might be differentiated. Values greater than 1.5 were considered indicative of human-sourced pollution (the actual ratio in human feces being around 5.5 and in ruminant feces about 0.25) (26). However, it is important to note that, when applied to archaeological and paleoenvironmental studies, the concentration of epi-5β-stanols must complement concentrations of each respective fecal stanol, as the sum of each respective compound pair can correct for the natural conversion of the 5β-stanol to its epimer (30). Therefore, in this study, we use a modified version of the coprostanol:5β-stigmastanol ratio, which includes each respective 5β-stanol epimer: (coprostanol + epi-coprostanol)/(5β-stigmastanol + epi-5β-stigmastanol).

We found the coprostanol/5β-stigmastanol ratio to be <0.25 before 2,250 cal y BP, indicating a source that was only from ruminant animals with negligible human input. After 2,250 cal y BP, the ratio exceeds the normal value for ruminant feces, which provides further evidence for an increase in human presence in the catchment (Fig. S2).

Correlating Temperature and Fecal 5B-Stanol Records. Correlation between the Lilandsvatnet coprostanol and Torneträsk reconstructed July temperature (31) was determined by applying a smooth fit, sixth-order polynomial negative exponential smoother, with a 0.1 sampling proportion at 100 intervals to both data sets using SigmaPlot, version 11.0 (Fig. 5*A*). Smooth fit data allowed both data sets to be compared at equal time steps and the correlation (r) between the data sets to be calculated. Ages for the smooth fit coprostanol data were lagged at 10-y increments from 0 to 160 and correlation coefficients were determined between each coprostanol time set and reconstructed temperature (Fig. 5*B*). The highest correlation between the two series is when the smooth fit coprostanol data are shifted by 80 y, which is within the 2σ (95% confidence range) of the chronological uncertainty (Fig. 5*C*). The calculated correlation coefficient for the 80-y lag coprostanol time set of 0.512 indicates a statistically significant relationship between the two records and implies a direct relationship between temperature and human feces deposition.

1. Stuiver M, Reimer PJ (1993) Extended ^{14}C data base and revised CALIB 3.0 ^{14}C age calibration program. *Radiocarbon* 35:215.
2. Reimer PJ, et al. (2009) IntCal09 and Marine09 radiocarbon age calibration curves, 0–50,000 years CAL BP. *Radiocarbon* 51:1111–1150.
3. Hall VA, Pilcher JR (2002) Late Quaternary Icelandic tephras in Ireland and Great Britain: Detection, characterization and usefulness. *Holocene* 12:223–230.
4. Hunt JB, Hill PG (1993) Tephra geochemistry: A discussion of some persistent analytical problems. *Holocene* 3:271–278.
5. Oldfield F, et al. (1997) Radiocarbon dating of a recent high-latitude peat profile: Stor Å myran, northern Sweden. *Holocene* 7:282–290.
6. Boygle J (2004) Towards a Holocene tephrochronology for Sweden: Geochemistry and correlation with the North Atlantic tephra stratigraphy. *J Quat Sci* 19:103–109.
7. Davies SM, Elmquist M, Bergman J, Wohlfarth B, Hammarlund D (2007) Cryptotephra sedimentation processes within two lacustrine sequences from West central Sweden. *Holocene* 17:319–330.
8. Pilcher J, Bradley RS, Francus P, Anderson L (2005) A Holocene tephra record from the Lofoten Islands, Arctic Norway. *Boreas* 34:136–156.
9. Larsen G, Dugmore AJ, Newton AJ (1999) Geochemistry of historic silicic tephras in Iceland. *Holocene* 9:463–471.
10. Pilcher JR, Hall VA, McCormac FG (1996) An outline tephrochronology for the Holocene of the north of Ireland. *J Quat Sci* 11:485.
11. Pilcher JR, Hall VA, McCormac FG (1995) Dates of Icelandic volcanic eruptions from tephra layers in Irish peats. *Holocene* 5:103–110.
12. Wastegård S, Björck S, Grauert M, Hanneon GE (2001) The Mjáuvøtn tephra and other Holocene tephra horizons from the Faroe Islands: A link between the Icelandic source region, the Nordic Seas and the European continent. *Holocene* 11:101–109.
13. Balascio NL, Wickler S, Narmo LE, Bradley RS (2011) Distal cryptotephra found in a Viking boathouse: The potential for tephrochronology in reconstructing the Iron Age in Norway. *J Archaeol Sci* 38:934–941.
14. Larsen G, Eirikısson J, Knudsen KL, Heinemeier J (2002) Correlation of late Holocene terrestrial and marine tephra markers, north Iceland: Implications for reservoir changes. *Polar Res* 21:283–290.
15. Collister JW, Rieley G, Stern B, Eglinton G, Fry B (1994) Compound-specific ^{13}C analyses of leaf lipids from plants with differing carbon dioxide metabolisms. *Org Geochem* 21:619–627.
16. Cranwell PA, Eglinton G, Robinson N (1987) Lipids of aquatic organisms as potential contributors to lacustrine sediments—II. *Org Geochem* 11:513–527.
17. Maffei M (1996) Chemotaxonomic significance of leaf wax alkanes in the Gramineae. *Biochem Syst Ecol* 24:53–64.
18. Grimalt J, Albaiges J (1987) Sources and occurrence of C12-C22 n-alkanes distributions with even carbon-number preference in sedimentary environments. *Geochim Cosmochim Acta* 51:1379–1384.
19. Ficken KJ, Li B, Swain DL, Eglinton G (2000) An n-alkane proxy for the sedimentary input of submerged/floating freshwater aquatic macrophytes. *Org Geochem* 31:745–749.
20. Meyers PA (2003) Applications of organic geochemistry to paleolimnological reconstructions: A summary of examples from the Laurentian Great Lakes. *Org Geochem* 34:261–289.
21. Cranwell PA (1973) Chain length distribution of n-alkanes from lake sediments in relation to post-glacial environmental change. *Freshw Biol* 3:259–265.
22. Fisher E, Wake R, Oldfield F, Boyle J, Wolff GA (2003) Molecular marker records of land use change. *Org Chem* 34:105–119.
23. Lima ALC, Farrington JW, Redd CM (2005) Combustion-derived polycyclic aromatic hydrocarbons in the environment: A review. *Environ Forensics* 6:109–131.
24. Eide I, et al. (2010) Polycyclic aromatic hydrocarbons in dated freshwater and marine sediments along the Norwegian coast. *Water Air Soil Pollut* 218:387–398.
25. Finkelstein DB, Pratt LM, Curtin TM, Brassell SC (2005) Wildfires and seasonal aridity recorded in Late Cretaceous strata from south-eastern Arizona, USA. *Sedimentology* 52:587–599.
26. Bull ID, Lockheart MJ, Elhmmali MM, Roberts DJ, Evershed RP (2002) The origin of faeces by means of biomarker detection. *Environ Int* 27(8):647–654.
27. Leeming R, Ball A, Ashbolt N, Nichols P (1996) Using faecal sterols from humans and animals to distinguish faecal pollution in receiving waters. *Water Res* 30: 2893–2900.
28. Sherwin MR, Van Vleet ES, Fossato VU, Dolci F (1993) Coprostanol (5β-cholestan-3b-ol) in lagoonal sediments and mussels of Venice, Italy. *Mar Pollut Bull* 26:501–507.
29. Evershed RP, Bethell PH (1996) Application of multimolecular biomarker techniques to the identification of fecal material in archaeological soils and sediments. *Archaeol Chem* 625:157–172.
30. Simpson IA, Bryant RG, Tveraabak U (1998) Relict soils and early arable land management in Lofoten, Norway. *J Archaeol Sci* 25:1185–1198.
31. Grudd H, et al. (2002) A 7400-year tree-ring chronology in northern Swedish Lapland: Natural climatic variability expressed on annual to millennial timescales. *Holocene* 12: 657–665.

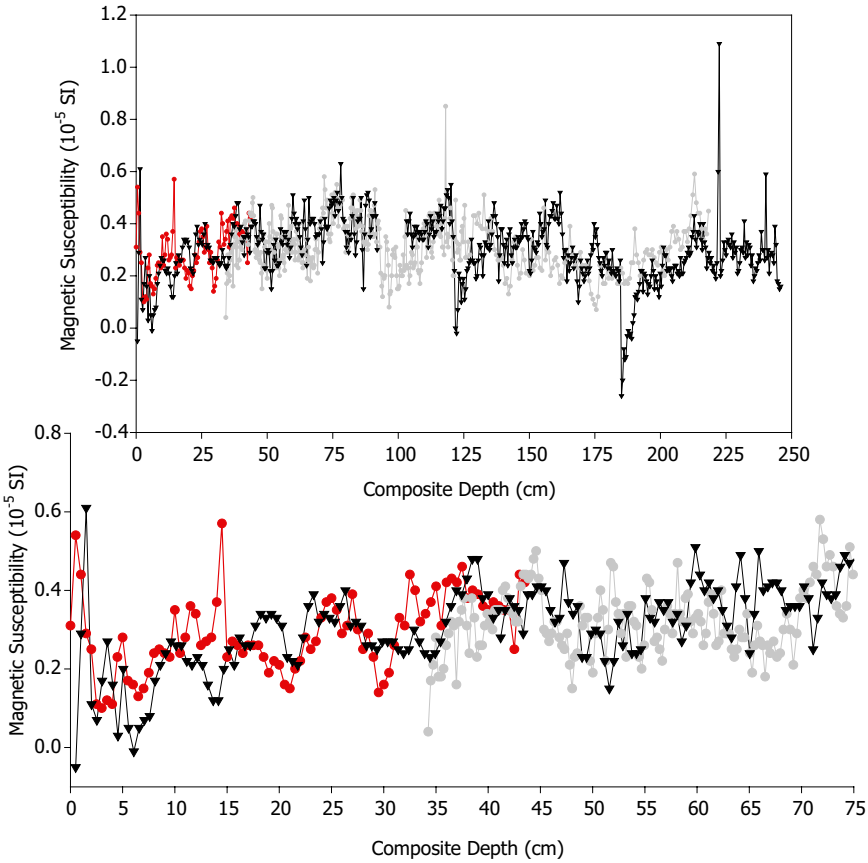

Fig. S1. Magnetic susceptibility (MS) profiles for sediment cores (LILA09, gray line; LILB09, black line; LILC09, red line). (*Upper*) MS records from all three cores placed on composite core depth. (*Lower*) Expanded view of the intersection between the 45-cm surface core (LILC09) and the longer cores (LILA09 and LILB09). Initially, the MS data were used to place cores on the same composite depth scale.

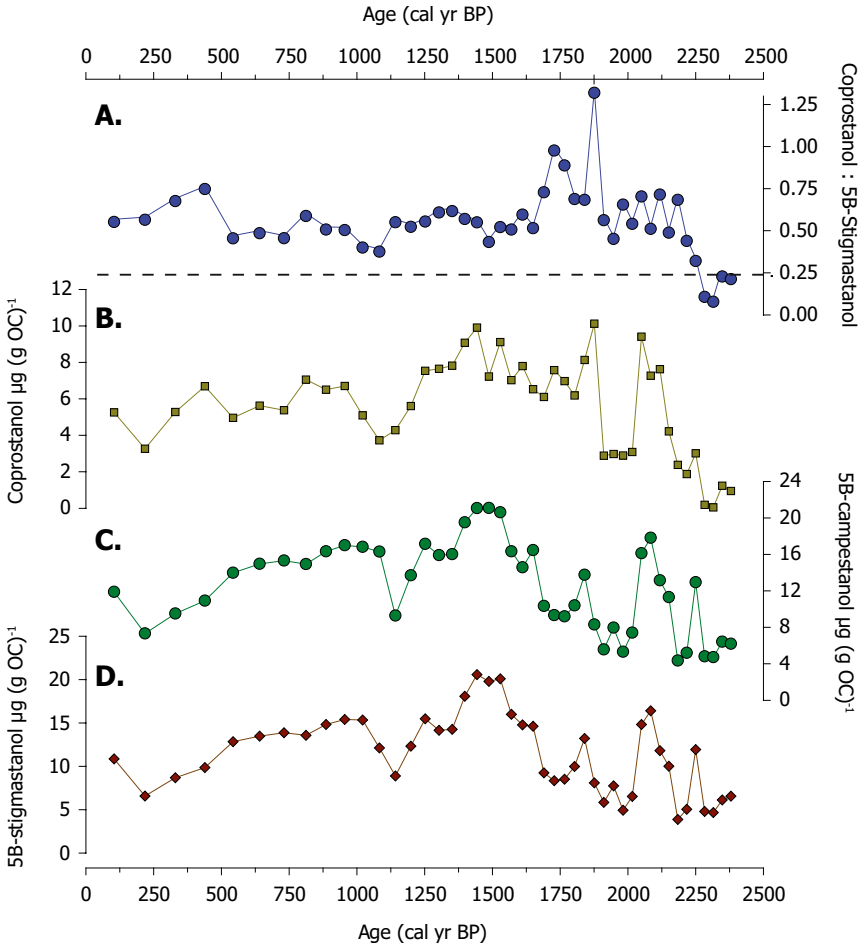

Fig. S2. Records of fecal 5β-stanol indices and concentrations provide evidence for changes in human and grazing livestock living within the catchment. The coprostanol/5β-stigmastanol ratio modified from Evershed and Bethell (1) (*A*) is <0.25 before 2,250 cal y BP, indicating a source that was only from ruminant animals with negligible human input. After 2,250 cal y BP, the ratio exceeds the normal value for ruminant feces, which provides further evidence for an increase in human presence in the catchment. Records of fecal 5β-stanol concentrations [µg (g OC)$^{-1}$] from grazing livestock (*B* and *C*) and human sources (*D*) further substantiate the results from this fecal stanol index.

1. Evershed RP, Bethell PH (1996) Application of multimolecular biomarker techniques to the identification of fecal material in archaeological soils and sediments. *Archaeol Chem* 625: 157–172.

Table S1. Radiocarbon dates used for constructing the composite core age-depth model

Composite sample depth, cm	Core name	Laboratory ID	^{14}C age, y BP	95.4% (2σ), cal y BP	Mean weighted age, cal y BP	AD/BC
21–22	LILC09	UCI-89387	1,610 ± 20	1,419–1,540	1,476	474 AD
40–41	LILC09	UCI-89388	2,180 ± 25	2,146–2,301	2,225	275 BC
66–67	LILA09	OS-78337	2,570 + 30	2,539–2,787	2,732	782 BC
125–126	LILA09	OS-78338	4,190 + 30	4,658–4,828	4,848	2898 BC
221–222	LILB09	OS-78339	6,200 + 35	7,023–7,165	7,084	5134 BC

Table S2. Average microprobe determined major element chemistry of tephras from Lilandsvatnet, Lofoten Islands

	SiO_2	TiO_2	Al_2O_3	MgO	CaO	MnO	FeO	Na_2O	K_2O	Cl	Total
0–1 cm											
LILC09-1—similar to ASKJA 1875 (*n* = 5)											
Average	72.32	0.85	12.79	0.68	2.44	0.12	3.54	3.54	2.27	0.06	98.78
SD	0.48	0.09	0.79	0.03	0.08	0.02	0.43	0.33	0.13	0.05	0.59
ASKJA 1875 (refs. 1 and 2) (*n* = 35)											
Average	72.24	0.83	12.63	0.68	2.39	0.11	3.52	3.46	2.40	—	98.22
SD	0.92	0.07	0.48	0.07	0.20	0.03	0.31	0.20	0.11	—	1.03
6–7 cm											
LILC09-7—similar to Hekla 1158 (*n* = 32)											
Average	66.61	0.49	14.33	0.41	2.96	0.24	5.84	4.32	2.26	0.06	97.65
SD	0.97	0.03	0.49	0.07	0.20	0.04	0.31	0.38	0.11	0.01	1.19
Hekla 1158 (refs. 2 and 3) (*n* = 16)											
Average	67.36	0.49	14.62	0.45	3.10	0.20	5.70	4.48	2.29	—	98.64
SD	0.78	0.05	0.47	0.04	0.1	0.04	0.16	0.3	0.12	—	1.03
8–9 cm											
LILC09-9A—similar to Hekla 1104 (*n* = 21)											
Average	70.52	0.23	13.81	0.09	2.02	0.14	3.29	4.47	2.54	0.07	97.24
SD	0.92	0.02	0.25	0.03	0.05	0.04	0.12	0.27	0.11	0.02	1.20
Hekla 1104 (refs. 2–5) (*n* = 114)											
Average	71.57	0.25	14.25	0.17	1.96	0.12	2.99	4.63	2.65	—	98.49
SD	1.38	0.09	0.49	0.14	0.27	0.02	0.42	0.3	0.24	—	1.57
LILC09-9B—similar to Hekla 1158 (*n* = 5)											
Average	67.04	0.47	14.29	0.36	3.06	0.21	5.64	4.23	2.20	0.06	97.69
SD	1.51	0.05	0.57	0.07	0.28	0.05	0.47	0.70	0.20	0.02	1.32
Hekla 1158 (refs. 2 and 3) (*n* = 16)											
Average	67.36	0.49	14.62	0.45	3.10	0.20	5.70	4.48	2.29	—	98.64
SD	0.78	0.05	0.47	0.04	0.1	0.04	0.16	0.3	0.12	—	1.03
26–27 cm											
LILC09-27—similar to SN-1 eruption of Snaefullljokulp (*n* = 13)											
Average	67.28	0.42	15.64	0.29	1.78	0.18	4.00	4.30	3.92	0.23	98.09
SD	0.72	0.07	0.46	0.09	0.24	0.04	0.17	1.13	0.20	0.03	1.20
SN-1 eruption of Snaefullljokulp ~1,780 ± 35 cal y BP (ref. 6) (*n* = 6)											
Average	67.27	0.38	15.66	0.33	1.72	—	4.08	5.07	4.36	—	98.96
SD	1.21	0.04	0.37	0.12	0.35	—	0.40	0.19	0.23	—	1.20
34–35 cm											
LILC09-35—similar to QUB-565 (*n* = 25)											
Average	68.82	0.45	13.90	0.20	1.33	0.17	4.38	5.32	3.93	0.21	98.77
SD	1.15	0.05	0.35	0.06	0.07	0.04	0.26	0.18	0.11	0.01	0.83
QUB 565 ~100–500 BC (ref. 7) (*n* = 18)											
Average	70.20	0.38	13.72	0.14	1.14	—	3.84	4.65	3.61	—	97.69
SD	1.43	0.11	0.61	0.12	0.38	—	0.58	0.37	0.19	—	2.10

Results are presented as oxides by stoichiometry and are not normalized. Totals below 95% were excluded from results.

1. Oldfield F, et al. (1997) Radiocarbon dating of a recent high-latitude peat profile: Stor Å myran, northern Sweden. *Holocene* 7:282–290.
2. Larsen G, Dugmore AJ, Newton AJ (1999) Geochemistry of historic silicic tephras in Iceland. *Holocene* 9:463–471.
3. Hall VA, Pilcher JR (2002) Late Quaternary Icelandic tephras in Ireland and Great Britain: Detection, characterization and usefulness. *Holocene* 12:223–230.
4. Pilcher JR, Hall VA, McCormac FG (1995) Dates of Icelandic volcanic eruptions from tephra layers in Irish peats. *Holocene* 5:103–110.
5. Pilcher JR, Hall VA, McCormac FG (1996) An outline tephrochronology for the Holocene of the north of Ireland. *J Quat Sci* 11:485.
6. Larsen G, Eirikısson J, Knudsen KL, Heinemeier J (2002) Correlation of late Holocene terrestrial and marine tephra markers, north Iceland: Implications for reservoir changes. *Polar Res* 21:283–290.
7. Pilcher J, Bradley RS, Francus P, Anderson L (2005) A Holocene tephra record from the Lofoten Islands, Arctic Norway. *Boreas* 34:136–156.